



## Article

# The Generation of Dual-Targeting Fusion Protein PD-L1/CD47 for the Inhibition of Triple-Negative Breast Cancer

Yanlin Bian <sup>1,†</sup>, Tong Lin <sup>1,†</sup>, Tanja Jakos <sup>1</sup>, Xiaodong Xiao <sup>2,3</sup> and Jianwei Zhu <sup>1,2,3,\*</sup>

<sup>1</sup> Engineering Research Center of Cell & Therapeutic Antibody, Ministry of Education, School of Pharmacy, Shanghai Jiao Tong University, Shanghai 200240, China; weixiaoby1@sjtu.edu.cn (Y.B.); lintong0802@163.com (T.L.); tanja.jakos@sjtu.edu.cn (T.J.)

<sup>2</sup> Jecho Biopharmaceuticals Co., Ltd., No. 2018 Zhongtian Avenue, Binhai New Area, Tianjin 300457, China; xiaodong.xiao@jecho.com

<sup>3</sup> Jecho Laboratories Inc., 7320 Executive Way, Frederick, MD 21704, USA

\* Correspondence: jianweiz@sjtu.edu.cn

† These authors contributed equally to this work.

**Abstract:** Triple-negative breast cancer (TNBC) is a highly aggressive subset of breast cancer with limited therapeutic options. However, its immune evasion mechanisms, characterized by the over-expression of the immune checkpoint molecules PD-L1 and CD47, can be targeted in order to facilitate cancer elimination by cells of innate and adaptive immunity. In this paper, we describe the design, preparation, and evaluation of three novel dual-targeting fusion proteins that were based on the structure frame of prototype IAB (innate and adaptive dependent bispecific fusion protein) and the “Orcutt-type IgG-scFv” molecular model. Three molecules with different spatial conformations were designed to improve antigen–antibody affinity by the addition of Ag–Ab binding sites from the variable region sequences of the anti-PD-L1 monoclonal antibody (mAb) atezolizumab and CV1, a high-affinity receptor of CD47. The results showed that the best-performing among the three proteins designed in this study was protein Pro3; its CV1 N-terminus and Fc domain C-terminus were not sterically hindered. Pro3 was better at boosting T cell proliferation and the engulfment of macrophages than the IAB prototype and, at the same time, retained a level of ADCC activity similar to that of IAB. Through improved design, the novel constructed dual-targeting immunomodulatory protein Pro3 was superior at activating the anti-tumor immune response and has thus shown potential for use in clinical applications.

**Keywords:** dual-targeting protein; PD-L1; CD47; TNBC; tumor inhibition



**Citation:** Bian, Y.; Lin, T.; Jakos, T.; Xiao, X.; Zhu, J. The Generation of Dual-Targeting Fusion Protein PD-L1/CD47 for the Inhibition of Triple-Negative Breast Cancer. *Biomedicines* **2022**, *10*, 1843. <https://doi.org/10.3390/biomedicines10081843>

Academic Editor: Satoshi Wada

Received: 23 June 2022

Accepted: 21 July 2022

Published: 30 July 2022

**Publisher’s Note:** MDPI stays neutral with regard to jurisdictional claims in published maps and institutional affiliations.



**Copyright:** © 2022 by the authors. Licensee MDPI, Basel, Switzerland. This article is an open access article distributed under the terms and conditions of the Creative Commons Attribution (CC BY) license (<https://creativecommons.org/licenses/by/4.0/>).

## 1. Introduction

Triple-negative breast cancer (TNBC) is a subtype of breast cancer (BC) that lacks the immunohistochemical expression of the estrogen receptor (ER), the progesterone receptor (PR), and the human epidermal growth factor receptor-2 (HER-2). TNBC has been characterized as highly aggressive and hard to treat; it has a poor prognosis [1] and represents approximately 10–19% of all breast cancer cases [2]. Distinct subpopulations of immune cells are known to have specific impacts on the function of the anti-tumor immune response. According to published reports [3–5], TNBC is associated with elevated intratumoral levels of both tumor-infiltrating lymphocytes (TILs) and tumor-associated macrophages (TAMs), along with a relatively high degree of expression of various immune checkpoints, such as programmed death ligand-1 (PD-L1) and CD47. Therefore, the need to restore the balance in the TNBC micro-environment provides a strong rationale for immunotherapies, especially for the use of the immune checkpoint blockade method.

Native regulatory mechanisms, including immune checkpoint pathways, have been investigated to prevent collateral damage from immune cells’ unrestrained activation. However, these same pathways can be exploited by tumors during immune evasion [6].

PD-L1 is an inhibitory ligand that is over-expressed by many human tumors. It can induce a negative signal of “do not find me” through engagement with its programmed death-1 receptor (PD-1) on the T lymphocyte surface, leading to reduced T cell proliferation, cytokine production, and cytotoxic functions [7,8]. Similarly, the increased expression of CD47 is involved in another tumor-evasion mechanism, in which interaction with its receptor signal regulatory protein- $\alpha$  (SIRP- $\alpha$ ) triggers an inhibitory “do not eat me” signal for phagocytic immune cells [9]. An increased understanding of the role of the immune system in tumor progression has revealed critical mechanisms by which TNBC escapes both innate and adaptive immunity; this knowledge provides the opportunity to target these inhibitory checkpoints.

Recent work has demonstrated the great potential of synergistic anti-tumor effects through the dual-blocking of the PD-1/PD-L1 and CD47/SIRP- $\alpha$  immune checkpoint pathways. For instance, avelumab, a fully human IgG1 anti-PD-L1 mAb, was shown to increase the secretion of interferon  $\gamma$  (IFN $\gamma$ ) from anti-tumor immune effector cells, which could enhance both PD-L1 expression and antibody-dependent cellular cytotoxicity (ADCC)-mediated lysis [10]. In addition, macrophages activated by the anti-CD47 antibody were able to initiate better T cell responses through enhanced CD8+ T cell cross-priming [11]. Furthermore, Liu’s [9] CD47/PD-L1 dual-targeting fusion protein (denoted as IAB) illustrated its synergistic functionality by activating both innate and adaptive immune responses in vivo. However, IAB had lower antigen–antibody affinity and bioactivity in vitro than its parental clones, mostly due to its single antigen–antibody (Ag–Ab) binding arm. This suggested that the enhancement of anti-TNBC cytotoxicity might be achieved through structural reconstruction by the addition of Ag–Ab binding sites.

A novel bispecific antibody format reconstructed by Orcutt et al. [12] was generated as a normal IgG1-like mAb; its light chains were fused, at the C-terminus, with scFv or peptides that recognized another antigen. This molecular model of an “Orcutt-type IgG-scFv” showed increased antigen affinity, good serum half-life, and an adequately stabilized structure [13].

Therefore, based on the specific immune signature of the TNBC tumor environment, where the immune checkpoint molecules CD47 and PD-L1 are over-expressed, we present here three novel dual-targeting fusion proteins for the treatment of TNBC. A schematic overview of the activity of the dual-targeting fusion protein in cancer is shown in Figure 1. Based on the structure frame of prototype IAB and the “Orcutt-type IgG-scFv” molecular model, we designed three novel proteins with different spatial conformations (denoted as Pro1, Pro2, and Pro3). Our improved design includes Ag–Ab binding sites from the variable region sequences of the anti-PD-L1 mAb atezolizumab [14] and from CD47’s high-affinity receptor CV1 [15]. Further, we performed a series of biochemical and biological activity assays to evaluate target binding affinities, tumor-directed cytotoxicity, ADCC, the stimulation of IFN- $\gamma$  secretion, and phagocytosis. This study was facilitated by the significant experience of the authors with protein–protein interactions [16], bispecific antibody platforms [17–19], and T-cell-engaging dual function anti-tumor molecules [20,21].

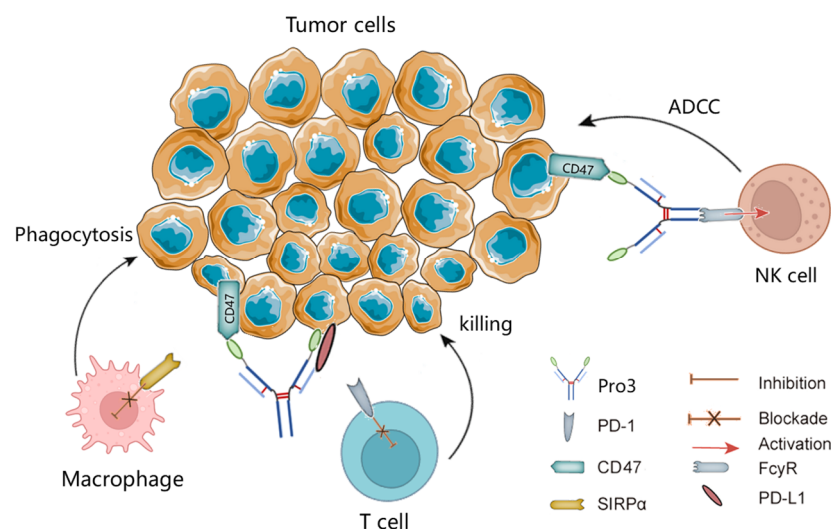


**Figure 1.** Schematic illustration of blockades of PD-L1 and CD47 by the dual-targeting fusion protein Pro3. ADCC, antibody-dependent cell-mediated cytotoxicity; NK, natural killer; SIRP $\alpha$ , signal-regulatory protein  $\alpha$ .

## 2. Materials and Methods

### 2.1. Strains, Cell Lines, and Other Reagents

The competent strain of *E. coli* DH5 $\alpha$  was produced in-house. The plasmids containing light and heavy chains of IgG1 Ab (pM09/CD3-L2 and pM09/5D9 Hc), variable regions of anti-human PD-L1 mAb atezolizumab (pET22b/PD-L1 scFv, pM09/PD-L1-Hc, and pM09/PD-L1-Lc), anti-PD-L1 scFv with cysteine mutation (pET22b/PD-L1 scFv\*), CD47-affinity receptor CV1 (pET22b/CV1, pM09/CV1-Fc, and pM09/Fc-CV1), and variable regions of anti-human CD47 mAb B6H12 (pUC57/B6H12-Lc and pUC57/B6H12-Hc) were all prepared from constructs stored at the Engineering Research Center of Cell & Therapeutic Antibody of MOE, China, at Shanghai Jiao Tong University (Shanghai, China).

The mammalian cell lines HEK293E and MDA-MB-231 (TNBC) were obtained from the American Type Culture Collection (ATCC, Rockville, MD, USA). The cell line MCF-10A (non-TNBC) was kindly gifted by Prof. Han Xianghui's group at Longhua Hospital (Shanghai, China). Human peripheral blood mononuclear cells (PBMCs) were obtained from the venous blood of healthy donors. Human macrophages, dendritic cells (DC), and CD4<sup>+</sup> T lymphocytes were all induced or isolated from fresh PBMCs.

The positive control antibodies anti-PD-L1 mAb (atezolizumab) and anti-CD47 mAb (B6H12) were produced in-house from previously stored plasmids: pM09/PD-L1-Hc and pM09/PD-L1-Lc, and pUC57/B6H12-Lc and pUC57/B6H12-Hc, respectively. The structure controls CV1-Fc and Fc-CV1 were obtained from the plasmids pM09/CV1-Fc and pM09/Fc-CV1, respectively. In addition, the prototype IAB was prepared according to the procedure outlined in published work [9].

### 2.2. Molecular Design and General Construction of Dual-Targeting Proteins

According to the structure frame of prototype IAB and the "Orcutt-type IgG-scFv" molecular model, three novel dual-targeting proteins of diverse spatial conformations were developed. They all contained symmetrical Ag-Ab binding sites with the variable region sequences of anti-PD-L1 mAb atezolizumab [14] and CD47's [15] high-affinity receptor CV1. The information about DNA sequences is provided in Appendix A.

Consistent with Orcutt's structure design, the CV1 was fused to the C-terminus of the light chain of the anti-PD-L1 IgG to create the novel protein Pro1, in which an intramolecular interchain disulfide bond (through cysteine mutation at VH G44C and VL Q100C) was introduced for higher molecular stability [12,13]. The heavy chain was the same as that of human IgG1, and the light chain was constructed as leader-VL\*-C $\kappa$ -(G<sub>4</sub>S)<sub>2</sub>-CV1, wherein

the VL\* was a variable light domain of atezolizumab, with a site mutation at Q100C. The novel proteins Pro2 and Pro3 were subsequently constructed by the fusion of CV1 at the C-terminus or N-terminus of anti-PD-L1 IgG; the heavy chain was VH-CH1-Fc-(G4S)4-CV1 (Pro2) or CV1-(G4S)2-VH-CH1-Fc (Pro3), and the light chain was the same as that of normal IgG1 for both proteins. All the fragments mentioned above were cloned into a separate pM09-vector. According to established protocols [12], the plasmids were transiently co-transfected into HEK293E cells by the polyethyleneimine (PEI) method [22] at the optimized weight ratios (Hc:Lc) of 1:1, 1:2, and 1:2, respectively, for Pro1, Pro2, and Pro3. The novel proteins Pro1, Pro2, and Pro3 were subsequently expressed and purified by MabSelect SURE chromatography (GE Healthcare, Shanghai, China) following the manufacturer's instructions. Detailed information about the construction of the novel dual-targeting proteins is provided in the Supplementary Materials (Figure S1 and Tables S1–S4).

### 2.3. Binding Analysis In Vitro

The dual-antigen binding affinities of the three novel proteins were evaluated by biolayer interferometry (BLI), which was conducted on a PALL ForteBio Octet RED96 system. The total working volume for the samples or buffers was 0.2 mL per well, and the working temperature was set at 37 °C. Briefly, streptavidin-coated biosensor tips were pre-wetted in phosphate-buffered saline (PBS), followed by the loading of the biotin-conjugated antigens PD-L1 or CD47 (100 nM, Sino Biological Inc., Beijing, China). Afterwards, a series of protein samples, including the positive controls (anti-PD-L1 mAb and anti-CD47 mAb), the prototype (IAB), and the three novel proteins (Pro1, Pro2, and Pro3), were associated with the ligands in concentrations of 25 nM, 50 nM, 75 nM, 100 nM, 125 nM, and 150 nM. Finally, the dissociation step was conducted by dipping the sensors in PBS. Analysis was performed with Octet software, during which the association and dissociation signals were baseline corrected, and global fit was used to calculate the affinity and rate constants. Accordingly, the association rate constant ( $k_a$ ) indicated the Ag–Ab complex formation rate per second in a 1 M solution, and the dissociation rate constant ( $k_d$ ) defined the stability of the Ag–Ab complex. The affinity constant  $K_D$  was calculated by the formula  $k_d/k_a$  [23,24].

### 2.4. PD-L1 and CD47 Co-Expression on MDA-MB-231 Cells

The co-expression of the antigens PD-L1 and CD47 on the TNBC cell line MDA-MB-231 was analyzed by flow cytometry. Tumor cells ( $5 \times 10^5$ ) were incubated with 1  $\mu$ g of anti-PD-L1 mAb or anti-CD47 mAb (both made in-house). FITC-conjugated anti-human Fc IgG (Jackson ImmunoResearch, West Grove, PA, USA) was used as the secondary antibody. Samples were measured on a CytoFLEX system (Beckman Coulter, Shanghai, China), and results were analyzed by CytExpert software (Beckman Coulter, Shanghai, China).

### 2.5. In Vitro Human Macrophage Activation

M1-type macrophages were induced in vitro from freshly isolated human PBMCs, with an initial treatment of M-CSF (Sino Biological Inc., Beijing, China) at a concentration of 25 ng/mL for 6 days and a subsequent exchange to a buffer containing a combination of M-CSF (25 ng/mL) plus IFN- $\gamma$  (50 ng/mL, Sino Biological Inc.) for an additional 24 h. Cells at  $1 \times 10^5$  cells/well of mature macrophages were co-plated with  $2 \times 10^5$  MDA-MB-231 cells. The cells were labeled with 1  $\mu$ M carboxyfluorescein diacetate succinimidyl ester (CFSE, Invitrogen, Wuhan, China) that was diluted in a serum-free RPMI 1640 medium (Gibco, Waltham, MA, USA) in a 48-well plate (Corning, Corning, NY, USA). Afterwards, 100 nM of antibodies (anti-CD47 mAb, CV1-Fc, Fc-CV1, IAB, Pro1, Pro2, and Pro3) or an IgG1 isotype control (Sino Biological Inc.) was added and incubated for 4 h at 37 °C. Next, the cells were washed in PBS and gently resuspended in TrypLE (Gibco, Waltham, MA, USA), followed by staining with 1  $\mu$ g of APC-conjugated anti-CD11b antibody (Bioscience). After the final washing step, all the samples were analyzed on a CytoFLEX system (Beckman Coulter), and the phagocytic index was calculated by GraphPad Prism 8 in accordance with the ratio of CFSE+ macrophages, as previously described [25].

### 2.6. Mixed Lymphocyte Reaction (MLR)

CD4<sup>+</sup> T cells were isolated from fresh PBMCs using a magnetic-bead cell separation kit (STEMCELL Technologies, Shanghai, China). DC cells were prepared by culturing PBMCs in vitro for 6 days with human IL-4 (20 ng/mL, Sino Biological Inc.) and GM-CSF (50 ng/mL, Peprotech, Cranbury, NJ, USA), followed by 24 h stimulation with lipopolysaccharides (LPS, 1 µg/mL). CD4<sup>+</sup> T cells ( $1 \times 10^5$ ) and mature DC cells ( $1 \times 10^4$ ) were co-cultured with control proteins (anti-PD-L1 mAb, CV1-Fc, Fc-CV1, and IAB) or the proteins Pro1, Pro2, and Pro3, with three concentrations for all three testing groups: 2.4 nM, 12 nM, and 60 nM. After 5 days, the secretion of cytokine IFN- $\gamma$  in cell culture supernatants was analyzed by ELISA (R&D systems, Minneapolis, MN, USA) as per the manufacturer's instructions.

### 2.7. Antibody-Dependent Cell-Mediated Cytotoxicity (ADCC)

The ADCC effect was evaluated using a lactate dehydrogenase (LDH) measurement kit (Promega, Durham, NC, USA), according to published work [26]. MDA-MB-231 cells expressing both PD-L1 and CD47 were seeded at a concentration of 5000 cells/100 µL in a 96-well plate. After 20 h, serially diluted controls (anti-PD-L1 mAb, CV1-Fc, Fc-CV1, and IAB) or the proteins (Pro1, Pro2, and Pro3), together with  $2 \times 10^5$  PBMCs per well, were added to the target cells and incubated for another 15 h. Afterwards, the LDH kit was utilized for the quantification of cytotoxicity mediated by antibodies in a colorimetric assay, where the measured absorbance was proportional to the fraction of lysed cells.

## 3. Results

### 3.1. Molecular Construction and Preparation of the Dual-Targeting Proteins

TNBC is a highly aggressive cancer with limited therapeutic options. However, it is characterized by high contents of both TILs and TAMs, along with over-expressed immune checkpoints, including PD-L1 and CD47; these characteristics suggest a strong rationale for immune checkpoint blockade therapy [3–5]. Recently, the anti-CD47/PD-L1 dual-targeting fusion protein IAB showed great potential for improving host immune responses in vivo [9], although it had sub-optimal antigen binding affinity and reduced biological activity in vitro on account of its “single-arm binding site”. In this study, based on the available information regarding the tumor-immune microenvironment in TNBC and the over-expression of the well-characterized immune checkpoints PD-L1 and CD47, we reconstructed the molecular frame of prototype IAB. Our aim was to enhance bioactivity through the addition of Ag–Ab binding sites, with reference to Orcutt's study [12], in which a novel format of bispecific Ab (bsAb) managed to retain both parental affinities and had good stability and in vivo half-life. Thereby, three novel dual-targeting proteins (Pro1, Pro2, and Pro3) that contained the variable region sequences of atezolizumab [14] and the CV1 monomer [15] were designed and developed; CV1 was fused to anti-PD-L1 IgG's Lc C-terminus and to the Hc C-terminus or N-terminus, respectively, as shown in Figure 2.

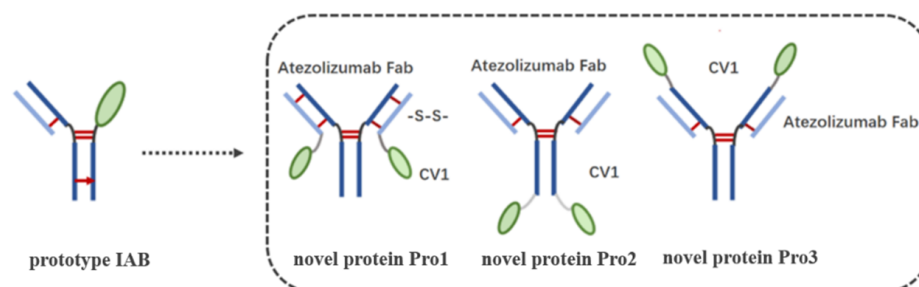


**Figure 2.** Design and schematic representation of the structures of the three dual-targeting proteins. The left “prototype IAB” is the structure of prototype IAB [12]. Prototype IAB was developed using “knobs into holes” technology, which is represented by a red arrow.

After transient expression by the PEI-mediated transfection of HEK293E cells, the three dual-targeting proteins were purified by MabSelect SURE chromatography and analyzed by SDS-PAGE under non-reducing and reducing conditions. As shown in Figure 3A,B, the molecular weight (MW) of Pro1 was in good agreement with the expected value of around 172 kDa for a fully assembled product; it also appeared to exhibit the desired purity. The yield of Pro1 was calculated as 43.4 mg/L by absorbance measurement, using the following formula:  $OD_{280}/\text{extinction coefficient}$  [27]. Likewise, Pro2 (173.2 kDa) and Pro3 (172 kDa) were both correctly assembled as full-length proteins with relatively high purity, yielding 26.5 mg/L and 17.3 mg/L, respectively. These results demonstrated that the novel dual-targeting proteins Pro1, Pro2, and Pro3 were successfully designed and prepared for further biological evaluations.

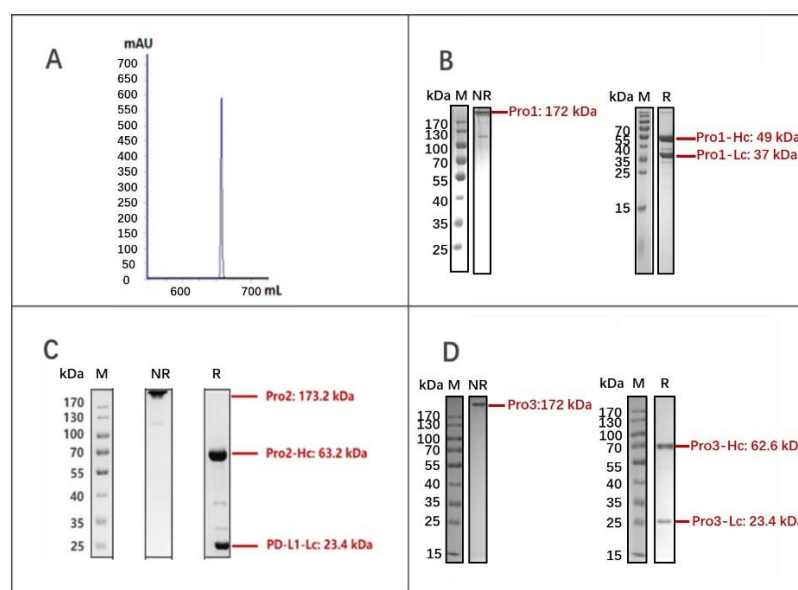


**Figure 3.** Expression and purification of dual-targeting fusion proteins. (A) Elution curve of Pro1 after MabSelect SURE purification; (B) SDS-PAGE analysis of Pro1 after affinity purification; (C) SDS-PAGE analysis of Pro2; (D) SDS-PAGE analysis of Pro3. (M: marker; NR: non-reduced samples; R: reduced samples).

### 3.2. Binding Characterization In Vitro

To confirm that the dual-antigen binding affinity of the reconstructed system was not disrupted by frame reconstruction, the affinities for PD-L1 and CD47 were measured by BLI assay using a ForteBio Octet RED96 system. The curves shown in Figure 4 are indicative of the antibodies' typical association and disassociation rates for the antigen PD-L1. According to the  $K_D$  constants calculated in Table 1, it was deemed that all of the three reconstructed formats with additional Ag–Ab binding sites did retain the parental affinity to PD-L1. All three proteins showed a significant increase in binding affinity as compared to the prototype IAB, among which Pro1 demonstrated the highest affinity ( $<1.0 \times 10^{-12}$ ).

**Table 1.** Rate and equilibrium constants of proteins binding to PD-L1.

Antibody	$K_a$ 1/Ms	$K_d$ 1/s	$K_D$ M	$R^2$
Anti-PD-L1 mAb	$1.82 \times 10^5$	$4.48 \times 10^{-6}$	$2.469 \times 10^{-11}$	0.9834
IAB	$9.50 \times 10^4$	$1.80 \times 10^{-4}$	$1.894 \times 10^{-9}$	0.9786
Pro1	$8.40 \times 10^4$	$1.0 \times 10^{-7}$	$<1.0 \times 10^{-12}$	0.9683
Pro2	$7.52 \times 10^4$	$2.85 \times 10^{-7}$	$3.794 \times 10^{-12}$	0.9861
Pro3	$7.21 \times 10^4$	$3.05 \times 10^{-7}$	$4.229 \times 10^{-12}$	0.9863

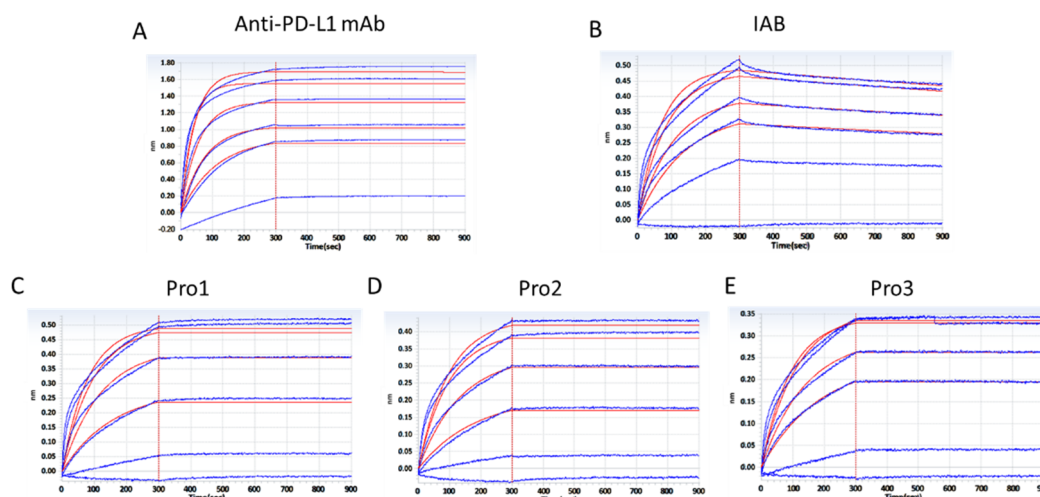


**Figure 4.** Affinity analysis of proteins binding to antigen PD-L1 through a BLI assay. (A) The positive control antibody; (B) prototype IAB; (C) Pro1; (D) Pro2; (E) Pro3. (Response units vs. time).

Accordingly, the association and disassociation rates of the controls and reconstructed proteins for the molecular target CD47 were measured, as presented in Figure 5.  $K_D$  constants, calculated in Table 2, showed that the three reconstructed formats exhibited similar affinities to CD47 compared to the parental antibody. The binding affinities of Pro1 ( $K_D = 9.138 \times 10^{-12}$ ) and Pro3 ( $K_D = 9.918 \times 10^{-12}$ ) were about 50-fold higher than that of IAB ( $K_D = 4.813 \times 10^{-10}$ ), but there was no significant improvement seen with Pro2.

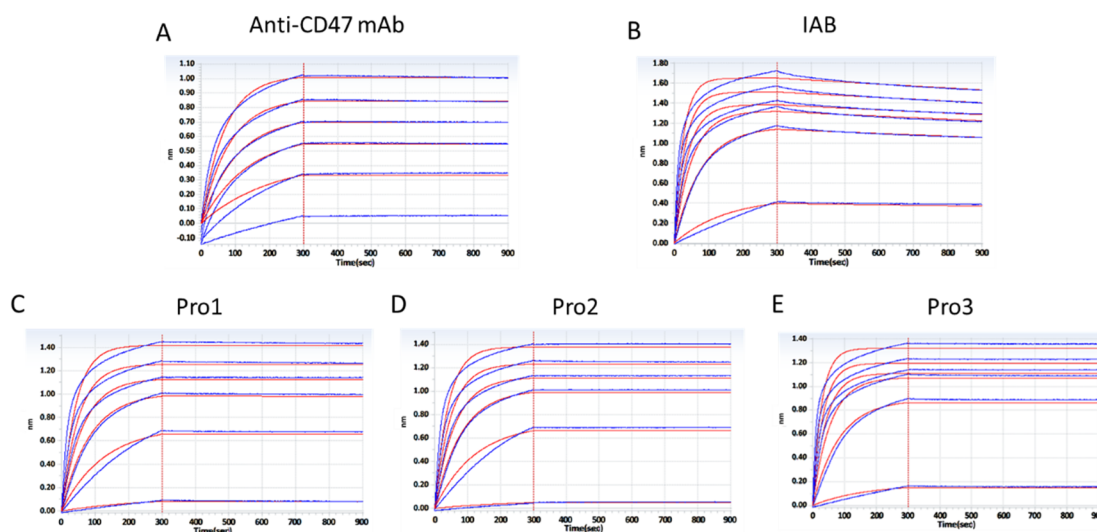


**Figure 5.** Affinity analysis of proteins to antigen CD47 through a BLI assay. (A) The positive control antibody; (B) prototype IAB; (C) Pro1; (D) Pro2; (E) Pro3. (Response units vs. time).

**Table 2.** Rate and equilibrium constants of antibodies binding to CD47.

Antibody	$K_a$ 1/Ms	$K_d$ 1/s	$K_D$ M	$R^2$
Anti-CD47 mAb	$9.79 \times 10^4$	$3.99 \times 10^{-7}$	$4.076 \times 10^{-12}$	0.9930
IAB	$2.57 \times 10^5$	$1.24 \times 10^{-4}$	$4.813 \times 10^{-10}$	0.9937
Pro1	$1.60 \times 10^5$	$1.46 \times 10^{-6}$	$9.138 \times 10^{-12}$	0.9954
Pro2	$1.65 \times 10^5$	$1.98 \times 10^{-6}$	$1.202 \times 10^{-11}$	0.9954
Pro3	$2.42 \times 10^5$	$2.40 \times 10^{-6}$	$9.918 \times 10^{-12}$	0.9919

### 3.3. Co-Expression of PD-L1 and CD47 on MDA-MB-231

Even though clinical immuno-histochemical analysis showed that TNBC was densely populated with TILs and TAMs, the immune cells were not able to effectively eliminate the transformed tumor cells. This fact can be largely attributed to the high expression of the inhibitory [3,4] immune checkpoints PD-L1 and CD47 [5]. Therefore, we investigated the dual-antigen expression on MDA-MB-231 cells to confirm whether this TNBC tumor cell line was qualified to be used in further bioassays. As shown in Figure 6, FACS analysis confirmed that MDA-MB-231 cells express both PD-L1 and CD47, which was consistent with the clinical pathology features of TNBC [28].

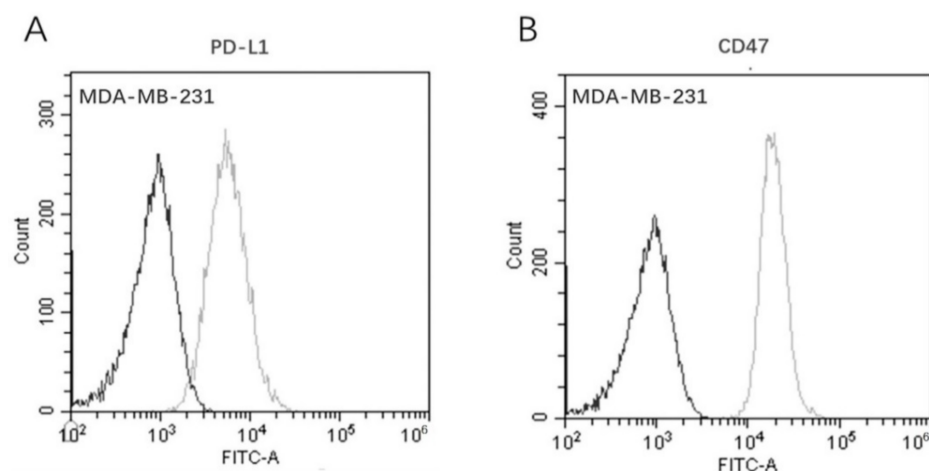


**Figure 6.** Co-expression of dual-targets on the TNBC cell line MDA-MB-231 by flow cytometry. (A) Antigen PD-L1; (B) antigen CD47. (Dark line: blank control; gray line: Ab-incubation group).

### 3.4. In Vitro Human Macrophage Activation

To explore how well the dual-targeting proteins induced phagocytosis, we used CFSE-labeled human TNBC tumor cells MDA-MB-231 and matured macrophages *in vitro*. The ratio of CFSE+ macrophages was calculated after incubation with 100 nM of control (IgG1 isotype, anti-CD47 mAb, CF1-Fc, and the prototype IAB) or dual-targeting proteins (Pro1, Pro2, and Pro3). As shown in Figure 7A–D, the positive controls anti-CD47 mAb and CV1-Fc, as well as prototype IAB, were able to induce macrophage-mediated phagocytosis to a significant extent. The phagocytosis mediated by the dual-targeting proteins was dependent on their spatial conformations. As indicated in Figure 7G, the novel protein Pro3, in which the Fc domain was not hindered by CV1, exhibited significantly improved bioactivity. Pro3 induced phagocytosis of MDA-MB-231 cells in 27.25%  $\pm$  1.51% of macrophages, as opposed to 18.06%  $\pm$  2.13% measured for IAB protein ( $p < 0.05$ ). Subsequently, Pro1, which had the Fc domain open but the N-terminus of CV1 blocked, performed similarly to IAB (Figure 7E); Pro2, in which both the Fc domain and N-terminus of CV1 were blocked, displayed much lower activity than the prototype (Figure 7F) ( $p < 0.05$ ). The above results demonstrated that the three reconstructed proteins induced human macrophages to phagocytize MDA-MB-231 tumor cells at different levels due to differences in the spatial structure of the antigen–antibody binding interface and the constant region. The best-performing protein was Pro3; its CV1 N-terminus and Fc domain C-terminus were not sterically hindered (Figure 7H).

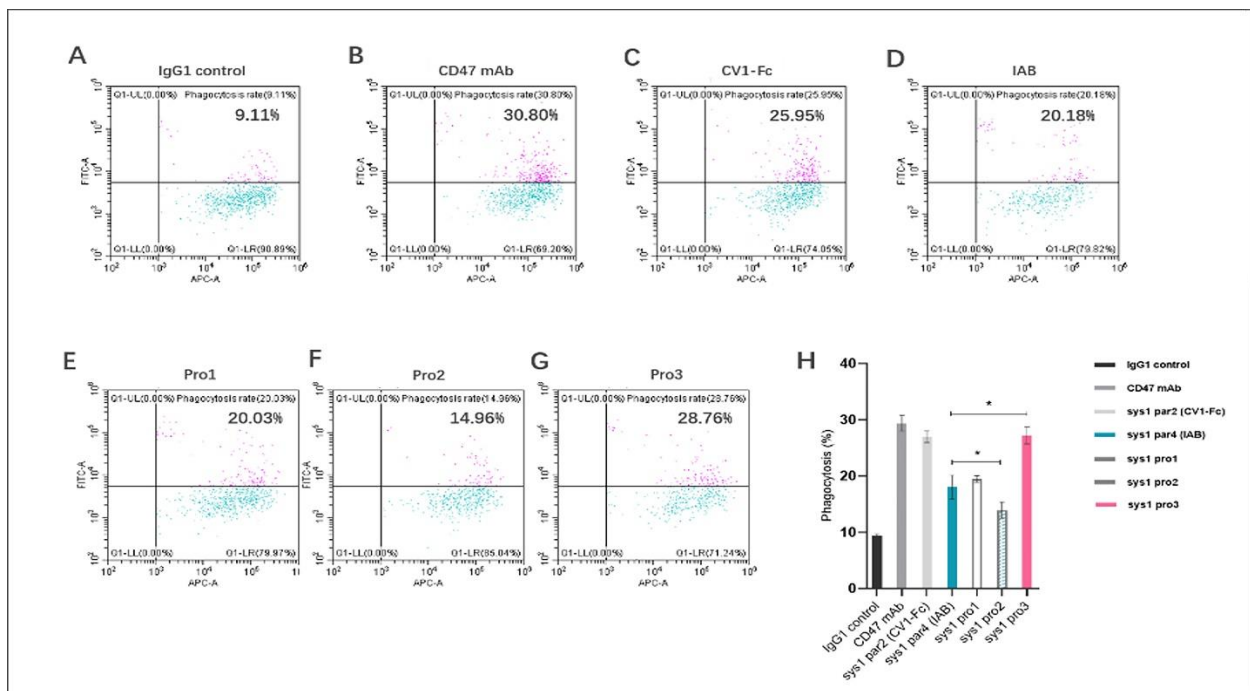


**Figure 7.** Novel reconstructed proteins induced human macrophages to phagocytize MDA-MB-231 tumor cells. The proportion of macrophages that engulfed tumor cells was measured by flow cytometry as a proportion of CFSE+CD11b+ cells. (A) Isotype IgG1; (B) positive control anti-CD47 mAb; (C) structure control CV1-Fc; (D) prototype IAI (E) Pro1; (F) Pro2; (G) Pro3. (H) The results are presented as mean ± standard deviation (SD), where \*  $p < 0.05$  is indicative of statistical difference.

### 3.5. Dual-Targeting Proteins Exhibited Superior Activity in a T Cell Activation Assay

The stimulation of T cells with the novel reconstructed proteins was evaluated in an allogeneic mixed lymphocyte reaction (MLR) system by using human CD4<sup>+</sup> T cells and DC cells that were isolated from PBMCs. As shown in Figure 8, PD-L1 blockade by anti-PD-L1 mAb, IAB, and all of the three proteins enhanced IFN- $\gamma$  release in a dose-dependent manner along a concentration range from 2.4 to 60 nM. The highest concentrations of IFN- $\gamma$  were released by the novel Pro3, which had the C-terminus of anti-PD-L1 mAb open and CV1 attached at the heavy chain N-terminus. A quantity of 60 nM of Pro3 stimulated the release of over 4000 pg/mL of inflammatory cytokine IFN- $\gamma$ . Owing to the exposed N-terminus of anti-PD-L1 mAb, Pro1 also induced a higher concentration of IFN- $\gamma$  than prototype IAB; however, Pro2, which had an open binding domain towards PD-L1 but blocked CV1, had lower activity when compared with IAB.

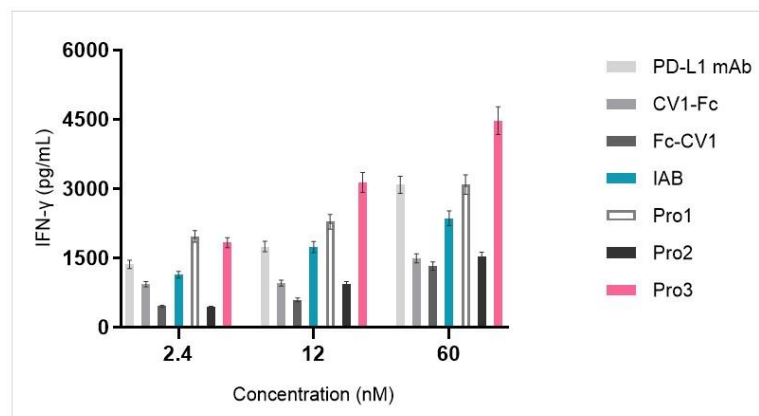


**Figure 8.** Dual-targeting proteins stimulated IFN- $\gamma$  release from the MLR system in a dose-dependent manner.

### 3.6. Dual-Targeting Proteins Retained the ADCC-Mediated Capacity of IAB

Although most of the fully human or humanized antibodies targeting PD-1 or PD-L1 are of the IgG4 isotype or mutated IgG1 Fc domain with low levels of ADCC activity [29], the anti-PD-L1 mAb avelumab can induce ADCC. Nevertheless, it was proved that avelumab administration was safe and did not trigger the lysis of PD-L1+ immune cells [30]. Furthermore, research confirmed that FcγRs' engagement could enhance the tumor inhibitory capability of the anti-PD-L1 antibody. Therefore, a combination of the normal IgG1 Fc domain and anti-PD-L1 mAb offers potential anti-tumor resistance. Here, the ability of the novel proteins to mediate ADCC activity in vitro was tested in an LDH assay.

As Figure 9A indicates, CV1-Fc had higher ADCC activity than anti-PD-L1 mAb, suggesting the former molecule can augment cytotoxicity towards MDA-MB-231 cells. Meanwhile, Fc-CV1, with the C-terminus of the heavy chain blocked, exhibited much lower cytotoxicity in comparison to CV1-Fc, for which the corresponding domain was kept free and open (17.59% vs. 42.95% for top cytotoxicity). The results further underline the importance of the correct spatial orientation of each part in the multi-domain assembly.

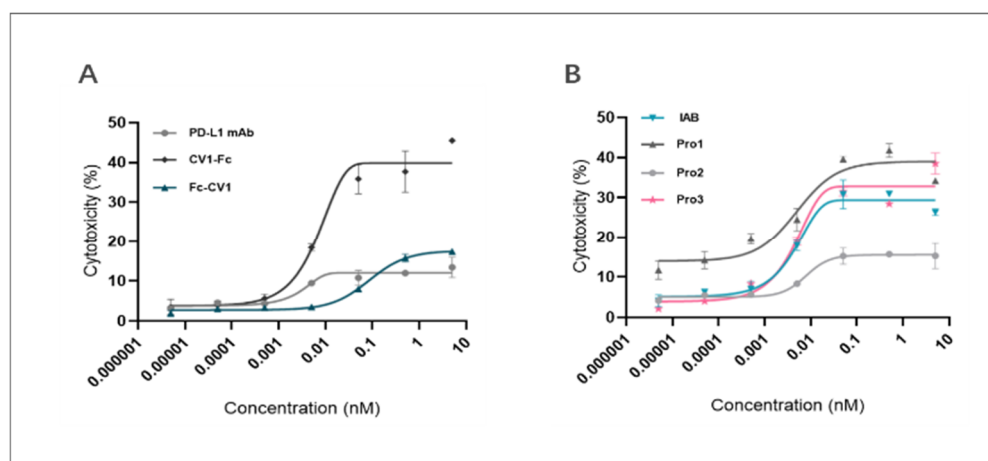


**Figure 9.** Reconstructed proteins and control proteins mediated ADCC against MDA-MB-231 cells. The plots show a dose-dependent increase in the proportion of lysed tumor cells for (A) controls (anti-PD-L1 mAb, CV1-Fc, Fc-CV1) and (B) reconstructed proteins (Pro1, Pro2, and Pro3).

The results of the ADCC activity test for the proteins are presented in Figure 9B and Table 3. In the concentration range from  $10^{-4}$  nM to  $10^{-1}$  nM, IAB, Pro1, and Pro3 all displayed significant ADCC-activating capability. When compared with the prototype, Pro1 showed relatively similar ADCC effects to Pro 3 on MDA-MB-231 cells (23.57% vs. 25.04% for the cytotoxicity span), while Pro2, at the same concentration gradient, showed a significant loss of activity (~5% to 29.36% vs. ~5% to 15.54% for the span). On the other hand, the ADCC effects of Pro3 were successfully retained, as the cytotoxicity span was 1.47 ~ 35.71%. These results suggest that the spatial format of Pro2 had a critical impact on Fc-mediated immune responses that was even more pronounced than that of the prototype. This illustrates, once again, that careful consideration of different spatial orientations is needed in order to achieve the desired functionality of reconstructed molecules.

**Table 3.** Dual-targeting proteins retained ADCC cytotoxicity towards MDA-MB-231 cells (E:T = 40:1).

Antibody	EC <sub>50</sub> (ng/mL)	Span (%)	R <sup>2</sup>
IAB	0.56	23.57	0.9666
Pro1	0.86	25.04	0.9194
Pro2	1.35	10.50	0.9468
Pro3	0.76	34.24	0.9599

#### 4. Discussion

TNBC has been characterized as highly aggressive, and it is harder to treat compared to other breast cancer subtypes [4]. However, the significant infiltration of both TILs and TAMs, along with the over-expression of immune checkpoints including PD-L1 and CD47, has provided a strong rationale for immune checkpoint blockade therapy [3–5]. In addition, published work [8] indicated that an anti-CD47/PD-L1 dual-targeting fusion protein IAB could restore the host's immune response *in vivo* by activating both innate and adaptive immunity for more effective tumor eradication. Nevertheless, the IAB could be improved further, as it has sub-optimal antigen-binding affinity and relevant bio-functions *in vitro* because of its "single-arm binding site". In order to enhance the bioactivity of the dual-targeting PD-L1/CD47 protein, we reconstructed the molecular frame of prototype IAB. The novel format provided additional Ag–Ab binding sites and, at the same time, exhibited sufficient molecular stability, as shown in another study by Orcutt et al. [12]. This format of bsAb managed to retain parental antibody affinities and had good stability or clearance *in vivo* [12]. Therefore, three novel dual-targeting proteins (denoted as Pro1, Pro2, and Pro3) that utilize the variable region sequences of atezolizumab [14] and the CV1 monomer [15] were developed, with a CV1-fusion at the anti-PD-L1 IgG's Lc C-terminus and the Hc C-terminus or N-terminus, respectively. Their multi-biological effects on the TNBC cell line MDA-MB-231 were studied to highlight the structure–activity relationship and provide preclinical data that would support their further development.

The data from our study indicated that dual-targeting proteins with additional Ag–Ab binding sites could mediate diverse levels of anti-TNBC activity, dependent on their different spatial conformations.

Published work highlighted the importance of specific sites at the N-terminus of the CV1 monomer for binding to its target CD47 [31]. The fusion of even short peptides at this site could significantly impact CV1's affinity and bioactivity [31]. Therefore, it was expected that the optimal affinity of our reconstructed proteins, which not only offer the benefits of CD47/SIRP $\alpha$  blockade but also of Fc-mediated phagocytosis, would require an unobstructed N-terminus of CV1. Simultaneously, the function of the Fc domain is critical for various stimulatory immune pathways (e.g., Fc/Fc $\gamma$ R I for mediating phagocytosis) [32]. Consistent with the evidence above, Pro3, with the CV1 N-terminus and the functional Fc domain exposed, exhibited significantly enhanced bioactivity, in terms of inducing the phagocytosis of MDA-MB-231 cells, in comparison to the prototype.

According to Wang's study [33], the expression of molecular PD-1 and PD-L1 were both upregulated in an allogeneic MLR system composed of CD4<sup>+</sup> T cells and DC cells. The relevant inhibitors of this pathway could enhance the release of pro-inflammatory cytokine. As we explored the influence of the novel proteins on T cell activity, we determined that all of the three novel proteins stimulated IFN- $\gamma$  release in a dose-dependent manner. Among them, Pro3, with an open C-terminus of anti-PD-L1 mAb and an open N-terminus of CV1, had the highest level of activity, with the highest concentrations of IFN- $\gamma$  released, reaching over 4000 pg/mL. Further, research by Soto-Pantoja [34] and Cui Lei [35] confirmed that CD47 was over-expressed on activated T lymphocytes and that they contributed to another inhibitory immune pathway of CD47/thrombospondin-1 (TSP-1). Its blockade by an anti-CD47 targeting drug also promoted the activation and proliferation of T cells. Therefore, along with the published evidence, our assumption about the disrupted spatial conformation of Pro2's CV1 monomer could explain its relatively low level of activity. The molecular conformation of IgG-like targeting antibodies was highly linked to their biological functions, such as ADCP; however, the situation was different, for example, for ADCC. It is believed that ADCC is mediated mainly through the Fc domain of CH2/CH3 binding to Fc/Fc $\gamma$ RIII expressed on NK cells. Orcutt-type proteins (the prototype of Pro1) have been reported to retain serological half-lives that are close to that of IgG mAbs through FcRn binding with the Fc domain of CH2/CH3 [36].

By performing an ADCC activity assay *in vitro*, we observed that CV1-Fc showed higher activity than anti-PD-L1 mAb. This is in accordance with the results evaluating

the co-expression of PD-L1 and CD47 on MDA-MB-231 cells, which showed a higher MFI for antigen CD47, suggesting that CD47 might dominate in a cytotoxicity model with MDA-MB-231 cells. The ratio of effector cells to target cells might explain the relatively narrow cytotoxicity span of the anti-PD-L1 mAb [37]. Furthermore, as ADCC activity depends on Ag–Ab binding affinity [37] along with the spatial constraints of functional Fc [32], the reconstructed format of Pro3 with an open CV1 N-terminus and an open Fc domain had the best bioactivity in this assay as well.

Our results comprehensively showed that, for leveraging the immune system to treat TNBC, the novel reconstructed proteins displayed markedly improved biological activity. They were designed by combining the structure frame of prototype IAB and the “Orcutt-type IgG-scFv” molecular model, with different spatial conformations taken into account. Among the proteins tested, Pro3 enhanced the engulfment of macrophages and T cell activation and, at the same time, retained a similar level of ADCC as the original molecule IAB. Herein, we describe the development of a novel candidate for an anti-cancer drug, namely Pro3, which offers improved inhibitory potential against TNBC cancer cells.

Recently, a variety of studies confirmed the synergistic anti-tumor effects of the simultaneous activation of both innate and adaptive immunity through multiple cross-priming mechanisms. For instance, the therapeutic efficacy of the anti-HER2/neu antibody [38] and of the anti-EGFR mAb cetuximab [39] partially depends on both natural killer cells and T cells. Moreover, atezolizumab, in combination with nab-paclitaxel, extended the progression-free survival (PFS) of TNBC patients [38], providing a strong rationale for exploring new therapeutic combinations for controlling tumors that are resistant to first-generation antibodies.

A study indicated that the dual blockade of CD47 and PD-L1 overcomes innate and adaptive immune resistance to antibody immunotherapy and substantially enhances anti-tumor responses [40]. The combination of anti-CD47 and PD-1/PD-L1 has been studied by different research groups [41]. Currently, multiple clinical trials are in phase I or phase II, such as one using a combination of ALX148 and pembrolizumab in head and neck squamous cell carcinoma (NCT03013218) [42], one using IMM01 and tislelizumab in advanced solid tumors (CTR20220791), and one using Hu5F9-G4 with different immunotherapies [43]. Among them, Hu5F9-G4 (5F9, magrolimab) is a first-in-class monoclonal antibody that blocks CD47. In terms of treatment, 5F9 is being tested in different treatment schemes in combination with different immunotherapies targeting PD-1/PD-L1, including avelumab (NCT03558139) [44], pembrolizumab (NCT04788043 and NCT04854499) [45], and atezolizumab (NCT03922477 and terminated). More clinical research is needed to adequately confirm the security and efficacy of these combinations in clinical practice.

Co-targeting PD-1/PD-L1 and CD47 with mAb combinations showed increased anti-tumor responses in clinical studies. However, CD47 mAbs are hindered by ubiquitous CD47 expression, leading to rapid target-mediated clearance and safety concerns. Consequently, dual-targeting CD47xPD-L1 bsAbs, enabling the preferential inhibition of CD47 on PD-L1-positive cells, are being tested as an alternative approach [46]. There are currently a number of bispecific antibodies targeting CD47 and PD-1/PD-L1 for the treatment of patients with various kinds of cancers [47], such as HX009 (NCT04886271), IBI322 (NCT04338659), PF-07257876 (NCT04881045) [48], SG12473 (CTR20211029), etc. Among them, the anti-PD-1/CD47 bsAb HX009 developed by Hangzhou Hanx Biopharmaceuticals, Inc. to treat patients with advanced solid tumors, including gastric cancer, colorectal cancer, and liver cancer, has shown promising clinical data. The anti-tumor activities of this approach and the objective responses in multiple tumor types [49], along with the role of bsAb, are now undergoing further investigations in a phase Ib/II study (NCT04886271). Another candidate, named IBI322, is a recombinant anti-human CD47/PD-L1 bsAb developed by Innovent Biologics Co. Ltd. (Suzhou, China); it has demonstrated promising efficacy signals and a favorable safety and tolerability profile [50]. Several phase Ib trials have been conducted to further explore the safety and efficacy of IBI322 in multiple indications (NCT04338659, NCT04795128, and NCT04912466).

A non-clinical study indicated that CD47 targeted monotherapy, or a combination with anti-PD-L1, preserves T cell bioenergetics and anti-tumor function, resulting in a decreased TNBC tumor burden [51]. However, there are few relevant clinical trials of the above dual-targeting combination as applied to TNBC, so future research should consider the verification and exploration of the molecular and cellular mechanisms of the dual-blockade of the immune checkpoint pathways PD-1/PD-L1 and CD47/SIRP $\alpha$  by our novel reconstructed protein Pro3.

## 5. Conclusions

This work successfully achieved the generation of dual-targeting fusion proteins with anti-PD-L1/CD47 functions. We described the design, preparation, and evaluation of three novel dual-targeting fusion proteins (denoted as Pro1, Pro2, and Pro3) that were based on the structure frame of prototype IAB and the “Orcutt-type IgG-scFv” molecular model. The three molecules with different spatial conformations were designed to improve antigen–antibody affinity by the addition of Ag–Ab binding sites from the variable region sequences of anti-PD-L1 mAb atezolizumab and CV1, a high-affinity receptor of CD47. According to the *in vitro* analysis by biolayer interferometry, the novel reconstructed proteins with increased antigen binding sites all retained the molecular binding affinities targeting CD47 and PD-L1 and showed a significant improvement over prototype IAB. The multi-biological effects towards the TNBC cell line MDA-MB-231 demonstrated different levels of biofunctional mediation due to differences among the three constructs in the spatial structure of the antigen–antibody binding interface and the constant region. Pro3 was better at boosting T cell proliferation and the engulfment of macrophages than IAB prototype, and it retained a level of ADCC activity similar to that of IAB. In summary, the novel dual-targeting fusion protein Pro3 demonstrated stronger TNBC cancer cell inhibitory activity and has potential for clinical applications. Meanwhile, our findings provide a research basis for the structural modification and development of anti-tumor pharmaceuticals targeting multiple immune checkpoints.

**Supplementary Materials:** The following supporting information can be downloaded at: <https://www.mdpi.com/article/10.3390/biomedicines10081843/s1>, Figure S1: Molecular schematic and plasmid constructions of three dual-targeting proteins; Table S1: The construction of plasmid pM09/Pro1-Hc as the heavy chain of Pro1; Table S2: The construction of plasmid pM09/Pro1-Lc as the light chain of Pro1; Table S3: The construction of plasmid pM09/Pro2-Hc as the heavy chain of Pro2; Table S4: The construction of plasmid pM09/Pro3-Hc as the heavy chain of Pro3.

**Author Contributions:** Conceptualization, Y.B., T.L. and J.Z.; methodology, Y.B., T.L. and J.Z.; software, Y.B. and T.L.; validation, Y.B. and T.L.; formal analysis, Y.B.; investigation, T.L.; resources, X.X.; data curation, Y.B. and T.L.; writing—original draft preparation, Y.B. and T.L.; writing—review and editing, Y.B., T.J. and J.Z.; visualization, Y.B., T.J. and J.Z.; supervision, X.X. and J.Z.; project administration, J.Z.; funding acquisition, J.Z. All authors have read and agreed to the published version of the manuscript.

**Funding:** This research was funded by the National Natural Science Foundation of China (to J.Z., No. 81773621 and 82073751).

**Institutional Review Board Statement:** Not applicable.

**Informed Consent Statement:** Not applicable.

**Data Availability Statement:** The dataset supporting the conclusions of this article is included within the article.

**Acknowledgments:** We offer thanks for technical support from Jecho Biopharmaceuticals Co., Ltd., and Jecho Laboratories, Inc.

**Conflicts of Interest:** The authors declare no conflict of interest.

## Appendix A

### Appendix A.1. The DNA Sequence of Anti-PD-L1 mAb (Atezolizumab)

#### Variable Domain of the Heavy Chain

GAAGTGCAGTTGGTGGAGTCTGGGGGAGGCTTGGTACAGCCTGGCG  
 GATCCCTGA  
 GACTCTCCTGTGCAGCATCTGGATTCACCTTTTCCGATTCTTGGATTCACTGGGTC  
 CGGCAAGCTCCAGGGAAGGGCCTGGAGTGGGTTCGCATGGATTAG  
 TCCATATGGTGGTAGTAC  
 CTATTATGCGGACTCTGTGAAGGGCCGATTACCATCTCCGCGGACACCAGTAA  
 GAACACCGCTTATCTGCAAATGAACAGTCTGAGAGCTGAGGACACGGCCGTC  
 TATTACTGTGCGGAAGACACTGGCCAGGTGGCTTTGACTACTGGGGCCAGGGA  
 ACCCTGGTCACCGTCTCCTCT

#### Variable Domain of the Light Chain

GACATCCAGATGACCCAGTCTCCATCCTCACTGTCTGCATCTGTAGGAGA  
 CAGAGTCAC  
 CATCACTTGTCTGGGCGAGTCAGGACGTAAGCACCGCCGTAGCATGGTATCAGCA  
 GAAACCAGGTAAAGCCCCTAAGTTACTGATCTATTCCGCATCCTTCTT  
 GTATAGTGGGGTCCCATCAAGGTTTCAGCGGCAGTGGATCTGGGACAGATTTAC  
 TCTCACCATCAGCAGCCTGCAGCCTGAAGATTTT  
 GCAACTTATTACTGCCAACAGTATCTG  
 TACCACCCGGCAACTTTTGGCCAGGGGACCAAGGTTCGAGATCAAAGG

### Appendix A.2. The DNA Sequence of Anti-CD47 mAb (B6H12)

#### Variable Domain of the Heavy Chain

GAAATTGTGTTGACACAGTCTCCAGCCACCCTGTCTTTGTCTCCAGGG  
 GAAA  
 GAGCCACCCTCTCCTGCAGGGCCAGTCAGACTATTAGCGACTACTTACACTGGT  
 ACCAACAGAAACCTGGCCAGGCTCCCAGGCTCCTCATCAAATTT  
 GCATCCCAATCCATTTCTGGCATCCCAGCCAGGTTTCAGTGGCAGTGGGTCTGGG  
 ACAGACTTCACTCTCACCATCAGCAGCCTAGAGCCTGAAGATTTTGCAG  
 TTTATTACTGTCAGAATGGTCACGGCTTTCCTCGGACGTTTCGGCCAAGGGACCAA  
 GGTGGAAATCAAA

#### Variable Domain of the Light Chain

GACATCCAGATGACCCAGTCTCCATCCTCACTGTCTGCATCTGTAGGAGA  
 CAGAGTCAC  
 CATCACTTGTCTGGGCGAGTCAGGACGTAAGCACCGCCGTAGCATGGTATCAGCA  
 GAAACCAGGTAAAGCCCCTAAGTTACTGATCTATTCCGCATCCTTCTT  
 GTATAGTGGGGTCCCATCAAGGTTTCAGCGGCAGTGGATCTGGGACAGATTTAC  
 TCTCACCATCAGCAGCCTGCAGCCTGAAGATTTT  
 GCAACTTATTACTGCCAACAGTATCTG  
 TACCACCCGGCAACTTTTGGCCAGGGGACCAAGGTTCGAGATCAAAGG

### Appendix A.3. The Nucleic Acid Sequence of CV1

GAGGAGGAGCTGCAGATCATTCAGCCTGACAAGTCCGTGTTGGTT  
 GCAGCTGGAGAGA  
 CAGCCACTCTGCGCTGCACTATCACCTCTCTGTTCCCTGTGGGGCCCATCCAGTG  
 GTTCAGAGGAGCTGGACCAGGCCGGGTTTTAATCTACAATCAAC  
 GCCAGGGCCCGTTCCCCCGGTAACAAGTGTTCAGACACCACAAAGAGAAAC  
 AACATGGACTTTTCCATCCGCATCGGTAACATCACCCAGCAGATGCCGGCAC  
 CTACTACTG  
 TATCAAGTTCCGGAAAGGGAGCCCCGATGACGTGGAGTTTAAGTCTGGAGCAGG  
 CACTGAGCTGTCTGTGCGGCCAAACCCTCT

## References

1. Sorlie, T.; Perou, C.M.; Tibshirani, R.; Aas, T.; Geisler, S.; Johnsen, H.; Hastie, T.; Eisen, M.B.; van de Rijn, M.; Jeffrey, S.S.; et al. Gene expression patterns of breast carcinomas distinguish tumor subclasses with clinical implications. *Proc. Natl. Acad. Sci. USA* **2001**, *98*, 10869–10874. [[CrossRef](#)] [[PubMed](#)]
2. Abkevich, V.; Timms, K.M.; Hennessy, B.T.; Potter, J.; Carey, M.S.; Meyer, L.A.; Smith-McCune, K.; Broaddus, R.; Lu, K.H.; Chen, J.; et al. Patterns of genomic loss of heterozygosity predict homologous recombination repair defects in epithelial ovarian cancer. *Br. J. Cancer* **2012**, *107*, 1776–1782. [[CrossRef](#)]
3. Mittendorf, E.A.; Philips, A.V.; Meric-Bernstam, F.; Qiao, N.; Wu, Y.; Harrington, S.; Su, X.P.; Wang, Y.; Gonzalez-Angulo, A.M.; Akcakanat, A.; et al. PD-L1 Expression in Triple-Negative Breast Cancer. *Cancer Immunol. Res.* **2014**, *2*, 361–370. [[CrossRef](#)]
4. Yu, C.; Zhen, L.; Li, H.; Zhang, Y.; Zhang, Q. The correlations between expression of tumor associated macrophages and the prognostic significances in triple negative breast cancer. *Pract. Oncol. J.* **2017**, *31*, 1–6.
5. Edris, B.; Weiskopf, K.; Volkmer, A.K.; Volkmer, J.P.; Willingham, S.B.; Contreras-Trujillo, H.; Liu, J.; Majeti, R.; West, R.B.; Fletcher, J.A.; et al. Antibody therapy targeting the CD47 protein is effective in a model of aggressive metastatic leiomyosarcoma. *Proc. Natl. Acad. Sci. USA* **2012**, *109*, 6656–6661. [[CrossRef](#)]
6. Korman, A.J.; Peggs, K.S.; Allison, J.P. Checkpoint blockade in cancer immunotherapy. In *Advances in Immunology: Cancer Immunotherapy*; Allison, J.P., Franoff, G., Eds.; Elsevier Academic Press Inc.: San Diego, CA, USA, 2006; Volume 90, pp. 297–339.
7. Freeman, G.J.; Long, A.J.; Iwai, Y.; Bourque, K.; Chernova, T.; Nishimura, H.; Fitz, L.J.; Malenkovich, N.; Okazaki, T.; Byrne, M.C.; et al. Engagement of the PD-1 immunoinhibitory receptor by a novel B7 family member leads to negative regulation of lymphocyte activation. *J. Exp. Med.* **2000**, *192*, 1027–1034. [[CrossRef](#)]
8. Brown, J.A.; Dorfman, D.M.; Ma, F.R.; Sullivan, E.L.; Munoz, O.; Wood, C.R.; Greenfield, E.A.; Freeman, G.J. Blockade of programmed death-1 ligands on dendritic cells enhances T cell activation and cytokine production. *J. Immunol.* **2003**, *170*, 1257–1266. [[CrossRef](#)]
9. Liu, B.; Guo, H.; Xu, J.; Qin, T.; Guo, Q.; Gu, N.; Zhang, D.; Qian, W.; Dai, J.; Hou, S.; et al. Elimination of tumor by CD47/PD-L1 dual-targeting fusion protein that engages innate and adaptive immune responses. *MAbs* **2018**, *10*, 315–324. [[CrossRef](#)] [[PubMed](#)]
10. Boyerinas, B.; Jochems, C.; Fantini, M.; Heery, C.R.; Gulley, J.L.; Tsang, K.Y.; Schlom, J. Antibody-Dependent Cellular Cytotoxicity Activity of a Novel Anti-PD-L1 Antibody Avelumab (MSB0010718C) on Human Tumor Cells. *Cancer Immunol. Res.* **2015**, *3*, 1148–1157. [[CrossRef](#)]
11. Tseng, D.; Volkmer, J.P.; Willingham, S.B.; Contreras-Trujillo, H.; Fathman, J.W.; Fernhoff, N.B.; Seita, J.; Inlay, M.A.; Weiskopf, K.; Miyanishi, M.; et al. Anti-CD47 antibody-mediated phagocytosis of cancer by macrophages primes an effective antitumor T-cell response. *Proc. Natl. Acad. Sci. USA* **2013**, *110*, 11103–11108. [[CrossRef](#)]
12. Orcutt, K.D.; Ackerman, M.E.; Cieslewicz, M.; Quiroz, E.; Slusarczyk, A.L.; Frangioni, J.V.; Wittrup, K.D. A modular IgG-scFv bispecific antibody topology. *Protein Eng. Des. Sel.* **2010**, *23*, 221–228. [[CrossRef](#)]
13. Reiter, Y.; Brinkmann, U.; Lee, B.; Pastan, I. Engineering antibody Fv fragments for cancer detection and therapy: Bisulfide-stabilized Fv fragments. *Nat. Biotechnol.* **1996**, *14*, 7. [[CrossRef](#)]
14. McDermott, D.F.; Sosman, J.A.; Sznol, M.; Massard, C.; Gordon, M.S.; Hamid, O.; Powderly, J.D.; Infante, J.R.; Fasso, M.; Wang, Y.V.; et al. Atezolizumab, an Anti-Programmed Death-Ligand 1 Antibody, in Metastatic Renal Cell Carcinoma: Long-Term Safety, Clinical Activity, and Immune Correlates From a Phase Ia Study. *J. Clin. Oncol.* **2016**, *34*, 833–842. [[CrossRef](#)] [[PubMed](#)]
15. Weiskopf, K.; Ring, A.M.; Ho, C.C.; Volkmer, J.P.; Levin, A.M.; Volkmer, A.K.; Ozkan, E.; Fernhoff, N.B.; van de Rijn, M.; Weissman, I.L.; et al. Engineered SIRP $\alpha$  variants as immunotherapeutic adjuvants to anticancer antibodies. *Science* **2013**, *341*, 88–91. [[CrossRef](#)]
16. Zhu, J.; Kahn, C.R. Analysis of a peptide hormone-receptor interaction in the yeast two-hybrid system. *Proc. Natl. Acad. Sci. USA* **1997**, *94*, 13063–13068. [[CrossRef](#)] [[PubMed](#)]
17. Han, L.; Chen, J.S.; Ding, K.; Zong, H.F.; Xie, Y.Q.; Jiang, H.; Zhang, B.H.; Lu, H.L.; Yin, W.H.; Gilly, J.; et al. Efficient generation of bispecific IgG antibodies by split intein mediated protein trans-splicing system. *Sci. Rep.* **2017**, *7*, 11. [[CrossRef](#)] [[PubMed](#)]
18. Han, L.; Zong, H.F.; Zhou, Y.X.; Pan, Z.D.; Chen, J.; Ding, K.; Xie, Y.Q.; Jiang, H.; Zhang, B.H.; Lu, H.L.; et al. Naturally split intein Npu DnaE mediated rapid generation of bispecific IgG antibodies. *Methods* **2019**, *154*, 32–37. [[CrossRef](#)] [[PubMed](#)]
19. Zong, H.F.; Han, L.; Chen, J.; Pan, Z.D.; Wang, L.; Sun, R.; Ding, K.; Xie, Y.Q.; Jiang, H.; Lu, H.L.; et al. Kinetics study of the natural split Npu DnaE intein in the generation of bispecific IgG antibodies. *Appl. Microbiol. Biotechnol.* **2022**, *106*, 161–171. [[CrossRef](#)] [[PubMed](#)]
20. Pan, Z.; Chen, J.; Xiao, X.; Xie, Y.; Jiang, H.; Zhang, B.; Lu, H.; Yuan, Y.; Han, L.; Zhou, Y.; et al. Characterization of a novel bispecific antibody targeting tissue factor-positive tumors with T cell engagement. *Acta Pharm. Sin. B* **2022**, *12*, 1928–1942. [[CrossRef](#)] [[PubMed](#)]
21. Chen, J.; Pan, Z.D.; Han, L.; Zhou, Y.X.; Zong, H.F.; Wang, L.; Sun, R.; Jiang, H.; Xie, Y.Q.; Yuan, Y.S.; et al. A Novel Bispecific Antibody Targeting CD3 and Lewis Y with Potent Therapeutic Efficacy against Gastric Cancer. *Biomedicines* **2021**, *9*, 17. [[CrossRef](#)]
22. Ding, K.; Han, L.; Zong, H.F.; Chen, J.S.; Zhang, B.H.; Zhu, J.W. Production process reproducibility and product quality consistency of transient gene expression in HEK293 cells with anti-PD1 antibody as the model protein. *Appl. Microbiol. Biotechnol.* **2017**, *101*, 1889–1898. [[CrossRef](#)]
23. Wallner, J.; Lhota, G.; Jeschek, D.; Mader, A.; Vorauer-Uhl, K. Application of Bio-Layer Interferometry for the analysis of protein/liposome interactions. *J. Pharm. Biomed. Anal.* **2013**, *72*, 150–154. [[CrossRef](#)]

24. Katsamba, P.S.; Navratilova, I.; Calderon-Cacia, M.; Fan, L.; Thornton, K.; Zhu, M.D.; Vanden Bos, T.; Forte, C.; Friend, D.; Laird-Offringa, I.; et al. Kinetic analysis of a high-affinity antibody/antigen interaction performed by multiple Biacore users. *Anal. Biochem.* **2006**, *352*, 208–221. [[CrossRef](#)]
25. Sakakura, K.; Takahashi, H.; Kaira, K.; Toyoda, M.; Murata, T.; Ohnishi, H.; Oyama, T.; Chikamatsu, K. Relationship between tumor-associated macrophage subsets and CD47 expression in squamous cell carcinoma of the head and neck in the tumor microenvironment. *Lab. Investig.* **2016**, *96*, 994–1003. [[CrossRef](#)]
26. Broussas, M.; Broyer, L.; Goetsch, L. Evaluation of antibody-dependent cell cytotoxicity using lactate dehydrogenase (LDH) measurement. *Methods Mol. Biol.* **2013**, *988*, 305–317. [[CrossRef](#)]
27. Baldassare, J.J.; Henderson, P.A.; Fisher, G.J. Isolation and characterization of one soluble and 2 membrane-associated FORMS of phosphoinositide-specific phospholipase-C from human-platelets. *Biochemistry* **1989**, *28*, 6010–6016. [[CrossRef](#)]
28. DiNome, M.L.; Orozco, J.I.J.; Matsuba, C.; Manughian-Peter, A.O.; Ensenyat-Mendez, M.; Chang, S.C.; Jalas, J.R.; Salomon, M.P.; Marzese, D.M. Clinicopathological Features of Triple-Negative Breast Cancer Epigenetic Subtypes. *Ann. Surg. Oncol.* **2019**, *26*, 3344–3353. [[CrossRef](#)]
29. Stevenson, G.T. Three major uncertainties in the antibody therapy of cancer. *Haematologica* **2014**, *99*, 1538–1546. [[CrossRef](#)]
30. Hamilton, G.; Rath, B. Avelumab: Combining immune checkpoint inhibition and antibody-dependent cytotoxicity. *Expert Opin. Biol. Ther.* **2017**, *17*, 515–523. [[CrossRef](#)]
31. Liu, Y.; Tong, Q.; Zhou, Y.; Lee, H.-W.; Yang, J.J.; Bühring, H.-J.; Chen, Y.-T.; Ha, B.; Chen, C.X.J.; Yang, Y.; et al. Functional Elements on SIRP $\alpha$  IgV Domain Mediate Cell Surface Binding to CD47. *J. Mol. Biol.* **2007**, *365*, 680–693. [[CrossRef](#)]
32. Zhao, Y.R. *Construction and Characterization a New Fusion Protein Pro-SIRP $\alpha$* ; The Second Military Medical University: Shanghai, China, 2016.
33. Wang, C.Y.; Thudium, K.B.; Han, M.H.; Wang, X.T.; Huang, H.C.; Feingersh, D.; Garcia, C.; Wu, Y.; Kuhne, M.; Srinivasan, M.; et al. In Vitro Characterization of the Anti-PD-1 Antibody Nivolumab, BMS-936558, and In Vivo Toxicology in Non-Human Primates. *Cancer Immunol. Res.* **2014**, *2*, 846–856. [[CrossRef](#)] [[PubMed](#)]
34. Soto-Pantoja, D.R.; Terabe, M.; Ghosh, A.; Ridnour, L.A.; DeGraff, W.G.; Wink, D.A.; Berzofsky, J.A.; Roberts, D.D. CD47 in the Tumor Microenvironment Limits Cooperation between Antitumor T-cell Immunity and Radiotherapy. *Cancer Res.* **2014**, *74*, 6771–6783. [[CrossRef](#)] [[PubMed](#)]
35. Lei, C. *Effect of Self-Expression of SIRP $\alpha$ -Fc Fusion Protein on T Cell Function*; Zhejiang Sci-Tech University: Hangzhou, China, 2015.
36. Ying, T.; Ju, T.W.; Wang, Y.; Prabakaran, P.; Dimitrov, D.S. Interactions of IgG1 CH2 and CH3 Domains with FcRn. *Front. Immunol.* **2014**, *5*, 146. [[CrossRef](#)] [[PubMed](#)]
37. McCall, A.M.; Shahied, L.; Amoroso, A.R.; Horak, E.M.; Simmons, H.H.; Nielson, U.; Adams, G.P.; Schier, R.; Marks, J.D.; Weiner, L.M. Increasing the affinity for tumor antigen enhances bispecific antibody cytotoxicity. *J. Immunol.* **2001**, *166*, 6112–6117. [[CrossRef](#)]
38. Brahmer, J.R.; Tykodi, S.S.; Chow, L.Q.M.; Hwu, W.J.; Topalian, S.L.; Hwu, P.; Drake, C.G.; Camacho, L.H.; Kauh, J.; Odunsi, K.; et al. Safety and Activity of Anti-PD-L1 Antibody in Patients with Advanced Cancer. *N. Engl. J. Med.* **2012**, *366*, 2455–2465. [[CrossRef](#)]
39. Hugo, W.; Zaretsky, J.M.; Sun, L.; Song, C.; Moreno, B.H.; Hu-Lieskovan, S.; Berent-Maoz, B.; Pang, J.; Chmielowski, B.; Cherry, G.; et al. Genomic and Transcriptomic Features of Response to Anti-PD-1 Therapy in Metastatic Melanoma. *Cell* **2016**, *165*, 35–44. [[CrossRef](#)]
40. Sockolosky, J.T.; Dougan, M.; Ingram, J.R.; Ho, C.C.M.; Kauke, M.J.; Almo, S.C.; Ploegh, H.L.; Garcia, K.C. Durable antitumor responses to CD47 blockade require adaptive immune stimulation. *Proc. Natl. Acad. Sci. USA* **2016**, *113*, E2646–E2654. [[CrossRef](#)]
41. Kuo, T.C.; Chen, A.; Harrabi, O.; Sockolosky, J.T.; Zhang, A.; Sangalang, E.; Doyle, L.V.; Kauder, S.E.; Fontaine, D.; Bollini, S.; et al. Targeting the myeloid checkpoint receptor SIRP $\alpha$  potentiates innate and adaptive immune responses to promote anti-tumor activity. *J. Hematol. Oncol.* **2020**, *13*, 160. [[CrossRef](#)]
42. Lakhani, N.J.; Chow, L.Q.M.; Gainor, J.F.; LoRusso, P.; Lee, K.-W.; Chung, H.C.; Lee, J.; Bang, Y.-J.; Hodi, F.S.; Kim, W.S.; et al. Evorpacept alone and in combination with pembrolizumab or trastuzumab in patients with advanced solid tumours (ASPEN-01): A first-in-human, open-label, multicentre, phase 1 dose-escalation and dose-expansion study. *Lancet Oncol.* **2021**, *22*, 1740–1751. [[CrossRef](#)]
43. Jiang, Z.; Sun, H.; Yu, J.; Tian, W.; Song, Y. Targeting CD47 for cancer immunotherapy. *J. Hematol. Oncol.* **2021**, *14*, 180. [[CrossRef](#)]
44. Lakhani, N.J.; Patnaik, A.; Liao, J.B.; Moroney, J.W.; Miller, D.S.; Fleming, G.F.; Axt, M.; Wang, Y.V.; Agoram, B.; Volkmer, J.-P.; et al. A phase Ib study of the anti-CD47 antibody magrolimab with the PD-L1 inhibitor avelumab (A) in solid tumor (ST) and ovarian cancer (OC) patients. *J. Clin. Oncol.* **2020**, *38*, 18. [[CrossRef](#)]
45. Colevas, A.D.; Park, J.J.; Fang, B.; Shao, J.; U'Ren, L.; Odegard, J.; Lal, I.; Phan, M.; Thein, K.Z.; Adkins, D. A Phase 2 Study of Magrolimab Combination Therapy in Patients with Recurrent or Metastatic Head and Neck Squamous-Cell Carcinoma. *Int. J. Radiat. Oncol. Biol. Phys.* **2022**, *112*, e42–e43. [[CrossRef](#)]
46. Chauchet, X.; Pernarrieta, E.; Bosson, N.; Calloud, S.; Hellequin, L.; Legrand, M.; Viandier, A.; Richard, F.; Cons, L.; Malinge, P.; et al. CD47  $\times$  PD-L1 bispecific antibodies for cancer therapy. *J. Immunother. Cancer* **2021**, *9*, A287. [[CrossRef](#)]
47. Yang, Y.; Yang, Z.; Yang, Y. Potential Role of CD47-Directed Bispecific Antibodies in Cancer Immunotherapy. *Front. Immunol.* **2021**, *12*, 686031. [[CrossRef](#)]

48. Chen, S.-H.; Dominik, P.K.; Stanfield, J.; Ding, S.; Yang, W.; Kurd, N.; Llewellyn, R.; Heyen, J.; Wang, C.; Melton, Z.; et al. Dual checkpoint blockade of CD47 and PD-L1 using an affinity-tuned bispecific antibody maximizes antitumor immunity. *J. Immunother. Cancer* **2021**, *9*, e003464. [[CrossRef](#)]
49. Roohullah, A.; Ganju, V.; Zhang, F.; Zhang, L.; Yu, T.; Wilkinson, K.; Cooper, A.; de Souza, P. First-in-human phase 1 dose escalation study of HX009, a novel recombinant humanized anti-PD-1 and CD47 bispecific antibody, in patients with advanced malignancies. *J. Clin. Oncol.* **2021**, *39*, 2517. [[CrossRef](#)]
50. Wang, J.; Sun, Y.P.; Chu, Q.; Duan, J.C.; Wan, R.; Wang, Z.J.; Zhao, J.; Li, H.Y.; Guo, Y.M.; Chen, Y.L.; et al. Abstract CT513: Phase I study of IBI322 (anti-CD47/PD-L1 bispecific antibody) monotherapy therapy in patients with advanced solid tumors in China. *Cancer Res.* **2022**, *82* (Suppl. 12), CT513. [[CrossRef](#)]
51. Stirling, E.; Willey-Shelkey, E.; Wilson, A.; Skardal, A.; Triozzi, P.; Terabe, M.; Miller, L.; Soker, S.; Soto-Pantoja, D. 206 An immune-competent tumor organoid platform to test novel immune checkpoint combinations targeting the receptor CD47 in triple negative breast cancer. *J. Immunother. Cancer* **2020**, *8*, A121–A122. [[CrossRef](#)]